



USE OF HIGH PRESSURE STAGES IN THE DESIGN OF NEW AXIAL FANS FOR HIGH PERFORMANCE BLOCKS IN COAL ELECTRICITY POWER PLANTS

Vaclav CYRUS

*AHT Energetika Ltd, Podnikatelska 550,
19011 Praha 9-Bechovice, Czech Republic*

SUMMARY

Three high pressure axial flow fan stages with low hub/tip ratio of 0.5 and 0.6 were designed and verified on 600 mm diameter test rig. Rotor blade elements near the hub had high aerodynamic loading. New stage blading application was proposed in the design of one-stage flue gas fan, external diameter of 4.3 m and peripheral velocity of 168 m/s, with the objective of replacing the standard two-stage axial flow fan.

INTRODUCTION

Each modern boiler block in existing coal fired power stations has usually one or two air fans and one to three flue gas fans. At the present time, most of the boiler blocks are gradually being refurbished. New advanced blocks with electrical power output of 500 to 800 MWe are either at the proposal stage or being commissioned. Some power stations require only one flue gas fan and one air fan at the boiler block. Most of the world's fan manufacturing companies use conventional design flow and pressure coefficients within the range of $\varphi_D = 0.35$ to 0.45 and $\psi_D = 0.30$ to 0.40 . The hub/tip ratio is typically in the range of 0.48 to 0.60 . Application of such design, in modern power block conditions, results in the fan having two stages and relatively high peripheral velocity of 160 m/s to 180 m/s and external diameter of 4.0 m to 5.0 m.

High pressure fan stage blading was designed using the latest techniques relating to the axial compressors, e.g. Baumgarten et al [1], Cyrus et al [2], [3], Sheard [4]. Great deal of attention was given to the improvement of fan aerodynamic performance, e.g. Vad [5], Clement et al [6] and Cyrus et al [7], [8], using the results of in depth analysis of the flow mechanism in the fan blading, inlet chamber and exhaust diffuser with the application of the CFD codes.

Our paper focuses on two primary objectives. First objective was to carry out analysis of the fan stage design with high pressure coefficient and high aerodynamic loading of the rotor and stator blade rows under the condition of maintaining the maximum stage efficiency of 90 %. Our test data

relating to three new advanced model fan stages with external diameter of 600 mm were used. The hub/tip ratio was in the range of 0.5 to 0.6.

The second objective was to investigate new large size flue gas fan design for the power station block output of 660 MW with the aim to replace two-stage fan by one-stage fan. Equivalent peripheral velocity $u_t = 168$ m/s and external diameter $D_t = 4.3$ m were used for both machines. Efficiency of the full size axial flow fan was calculated on the basis of modelled stage test data using the Darmstadt TU similarity method [9].

AXIAL FLOW FAN KEY DESIGN PARAMETERS

Axial flow fans used in power stations consist of an inlet suction chamber, one or two axial flow stages and a diffuser (Fig.1). Typical fan aerodynamic characteristics are shown in Fig. 2. Gas volume flow rate is altered by turning the rotor blades. Fan efficiency contours are also shown.

Boiler designers usually prescribe several working points, e.g. 50%N, 100%N, BMCR and D. The highest fan efficiency should be at the nominal point of 100%N. Required maximum flow rate value Q is at the point D. This condition determines the electric motor maximum output.

Fig. 3 and Fig. 4 show set of graphs applicable for the parametric analysis of the principal fan parameters. These were derived from the definitions and relationships valid in the fan's internal aerodynamics. Relationship of the fan work Y and peripheral velocity u_t for the different pressure coefficient values $\psi_F = 0.4$ to 1.0 are presented in Fig. 3. It can be seen that for the relatively high work value used in modern fan design, $Y = 10,000$ J/kg, high pressure coefficient of $\psi_F = 0.8$ and peripheral velocity $u_t = 160$ m/s should be used.

Fig. 4 shows relationships of the volume flow rate Q and the fan external diameter D_t , flow coefficient ϕ and stage hub/tip ratio v . The hub/tip ratio $v = 0.5$ and 0.6 and flow coefficient $\phi = 0.4$ and 0.6 were selected as they relate to the advance fan design. The peripheral velocity of $u_t = 130$ m/s and $u_t = 170$ m/s relate to the older and modern design, respectively. It follows from Fig. 4, for example, that the maximum flow rate $Q = 1,000$ m³/s may be used in the axial flow fan design with the hub/tip ratio of $v = 0.6$, peripheral velocity $u_t = 170$ m/s and tip diameter $D_t = 4.35$ m at the flow coefficient of $\phi = 0.6$. If the flow coefficient $\phi = 0.4$ is used, then the external diameter is $D_t = 5.40$ m.

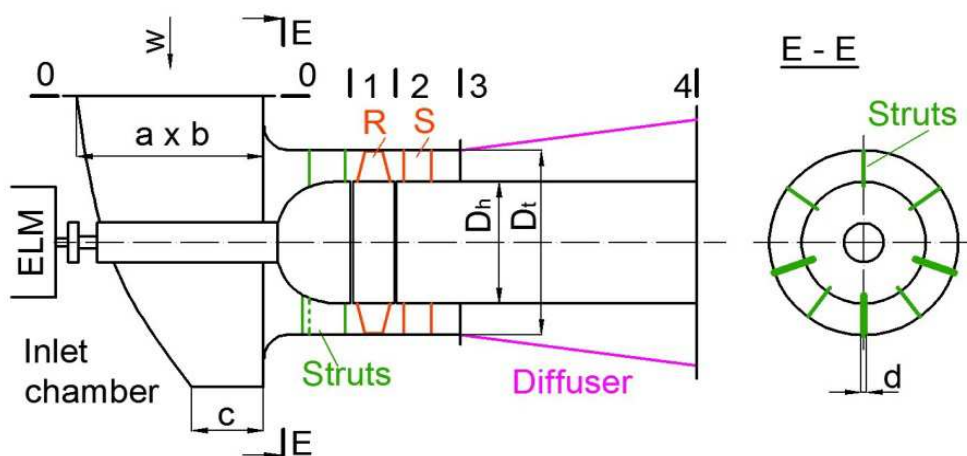


Figure 1: axial flow fan

EFFECT OF THE INLET CHAMBER AND DIFFUSER LOSSES ON THE AXIAL FLOW FAN AERODYNAMIC PERFORMANCE

Relationship of the aerodynamic performance of the fan stage blading (R+S) and the complete axial flow fan is derived in [3] and it is based on one-dimensional flow model. It assumes axial flow in the inlet and outlet fan stage Planes 1 and 3 (Fig.1). Equations (1) and (2) show that the fan efficiency η_F and pressure coefficient ψ_F decrease with the loss coefficients of the inlet chamber ζ_{IC} and the diffuser ζ_D and the flow coefficient ϕ

$$\eta_F/\eta_{ST} = 1 - (\zeta_{IC} + \zeta_D) \phi^2/\psi_{ST}, \quad (1)$$

$$\psi_F/\psi_{ST} = 1 - (\zeta_{IC} + \zeta_D) \phi^2/\psi_{ST}, \quad (2)$$

where the definitions of the following properties are:

$$\zeta_{IC} = (p_{T0} - p_{T1})/q_1 \text{ and } \zeta_D = (p_{T3} - p_{T4})/q_3 \quad (3)$$

$$q_1 = q_3 = 0.5\rho (Q/A_1)^2$$

$$\phi = Q/(A_1 u_t), \quad A_1 = \pi D_t^2 (1-v^2)/4. \quad (4)$$

This tendency is weakened by the increase of the fan's stage blading pressure coefficient ψ_{ST} . From the equations (1) and (2) it follows that the fan's operating points should be located within the performance field that has low flow coefficient in order to attain high fan efficiency η_F . Low energy loss condition in the fan's inlet and outlet parts is of crucial importance.

These conclusions are confirmed in Fig. 5, which shows two sets of curves valid for the sums of loss coefficients $\zeta_{IC} + \zeta_D = 0.15$ and 0.25 . The first set applies to good aerodynamic design of the inlet chamber and exhaust diffuser relating to modelled axial flow fan with the external diameter of 600 mm and hub/tip ratio of 0.6, which was theoretically and experimentally investigated by the authors of [7], [8]. The minimum evaluated values of loss coefficients ζ_{IC} and ζ_D were within range of $\zeta_{IC} = 0.11$ to 0.13 and $\zeta_D = 0.005$ to 0.006 , respectively. The values of ζ_D were determined at working points close to the design point, where the inlet velocity profiles were smooth and swirl was approximately zero. The sum of loss coefficients $\zeta_{IC} + \zeta_D = 0.25$ relates to the low cost fans with the inlet casing having simplified shape of flow channels.

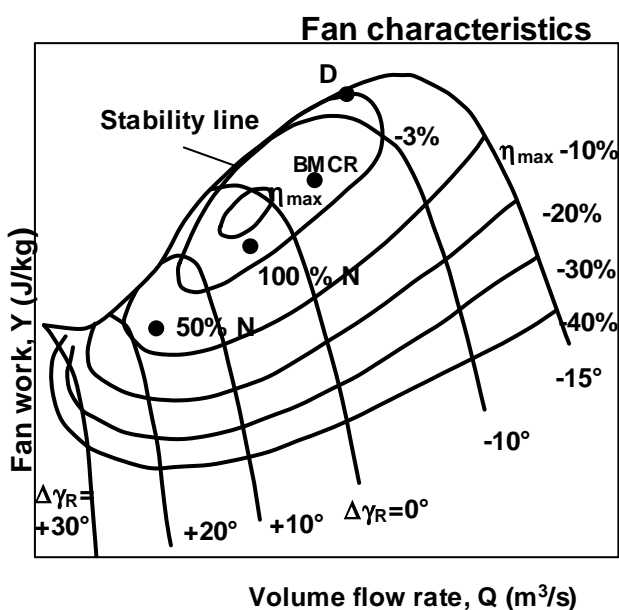


Figure 2: fan performance field

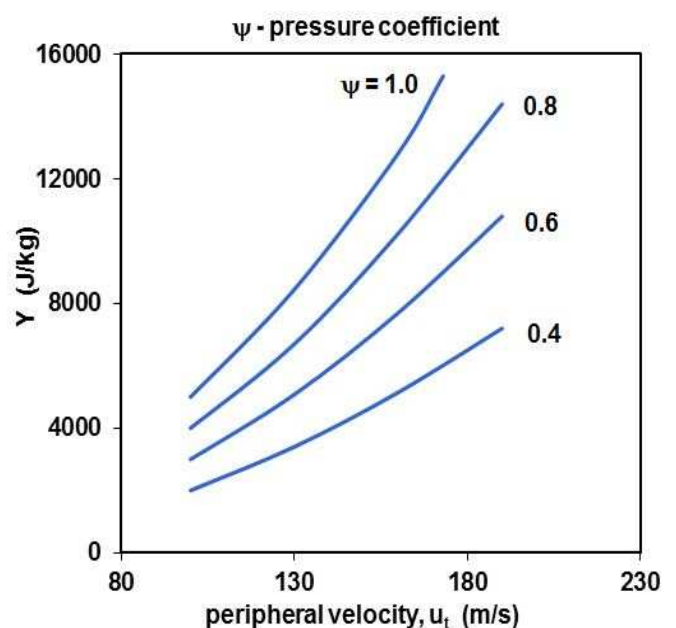


Figure 3 : dependence of fan work on peripheral velocity

Table 1: parameters of axial flow fan stages

Stage	v	φ_D	Ψ_D	Rotor blade row			Stator blade row		
				z_R	$\sigma_{R,h}$	AR_R	z_S	$\sigma_{S,h}$	AR_S
A	0.60	0.60	0.83	22	2.14	1.17	31	2.88	1.26
B		0.35	0.46	22	2.14	1.26	31	2.88	1.30
C	0.50	0.45	0.36	18	1.81	1.67	23	3.12	1.36
D	0.55	0.40	0.30	12	1.16	1.45	15	1.30	1.50

AXIAL FLOW FAN DESIGN

Design parameters of new fan axial stages

The axial fan stage geometry was derived using the CADAC design code for the axial flow compressor stage [11]. Axisymmetric flow solution is based on the streamline curvature method; the aerodynamic performance of the blade element is derived using the Lieblein's method [12] with secondary losses calculated for the blade with and without the tip clearance; refer to Cyrus [2]. Flow in the inlet and outlet planes is axial. The CFD method (NUMECA program [13]) was used to calculate the new stage aerodynamic performance.

The main parameters of new advanced stages with high aerodynamic loading, which were designed and tested in AHT Energetika Ltd, are presented in Table 1 and are denoted by the capital letters A, B and C. For the comparison data relating to the standard stage D with moderate aerodynamic loading are also presented.

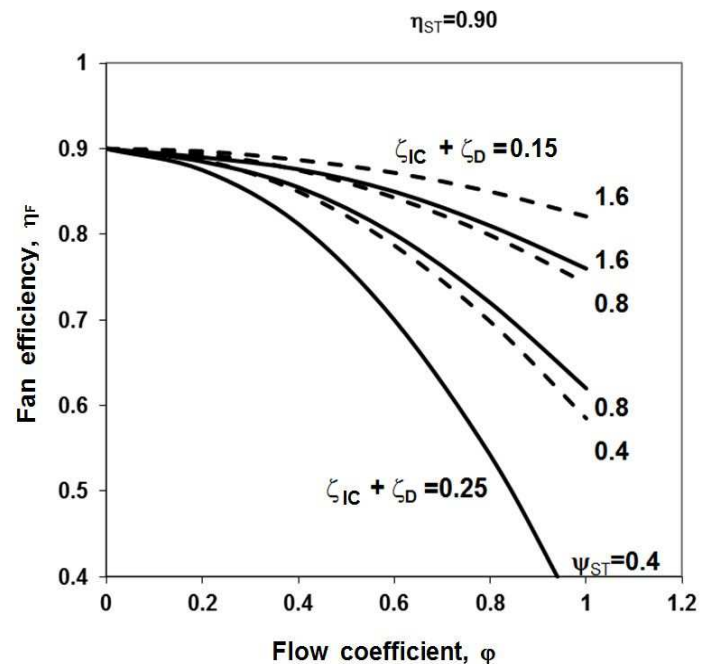
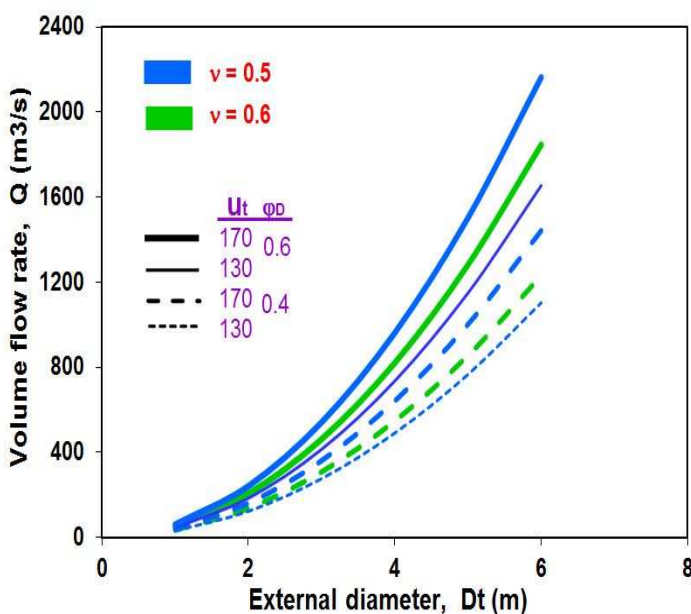


Figure 5: dependence of volume flow rate on external diameter

Figure 6: dependences for fan efficiency

Profiles of the rotor and stator airfoils were NACA 65th series with reinforced trailing edge. Camber lines were circular. In order to achieve acceptable aerodynamic loading of the rotor blade elements near the hub the smaller fan work redistribution along the radius was applied. The relative difference of the total enthalpy increase at the hub was lower than at the casing $(\Delta H_t - \Delta H_h) / \Delta H_m = 6\%$ and 8% for the Stage A and B, respectively. Work redistribution was zero for the Stage C and D.

The maximum number of rotor blades $z_{R,max}$ in stages A and B is given by the hub/tip ratio, in this case $z_{R,max} = 22$ and $\nu = 0.6$, and is related to the location of the rotor blades hydraulic turning mechanism in the fan hub. For this reason the number of rotor blades in the Stage C is lower: $z_R = 18$, the hub/tip ratio was $\nu = 0.5$. We note that the number of stator vanes is not usually restricted in the axial fan design.

Stage A had the design flow coefficient $\varphi_D = 0.60$ and design pressure coefficient $\psi_D = 0.83$. Stage B had the following parameters: $\varphi_D = 0.35$ and $\psi_D = 0.46$ (Table 1). For the Stage C the design pressure coefficient $\psi_D = 0.36$ was lower than for Stages A and B owing to the lower hub/tip ratio of $\nu = 0.50$.

The aerodynamic loading of the rotor and stator blade elements at the design point of three new stages A, B and C was relatively high. Diffusion factor was used as the criterion of cascade aerodynamic loading. All stages had the maximum values of the rotor and stator diffusion factor in the range of $DF = 0.55$ to 0.58 in the area near the hub, as it follows e.g. from the spanwise distributions of the rotor cascades diffusion factor valid for the described stages (Fig.6). In order to maintain these DF values on the hub of the stator blade elements, it was necessary to apply relatively high cascade solidity $\sigma_{s,h} = c/s = 2.9$ to 3.1 (Table 1).

The aerodynamic loading of the standard Stage D rotor and stator cascades was moderate as it is evident from Fig. 6. All investigated stage cascades had subcritical design diffusion factor of $DF < 0.60$ thus the studied stages achieved required maximum stage efficiency of $\eta_{ST,max} > 0.9$.

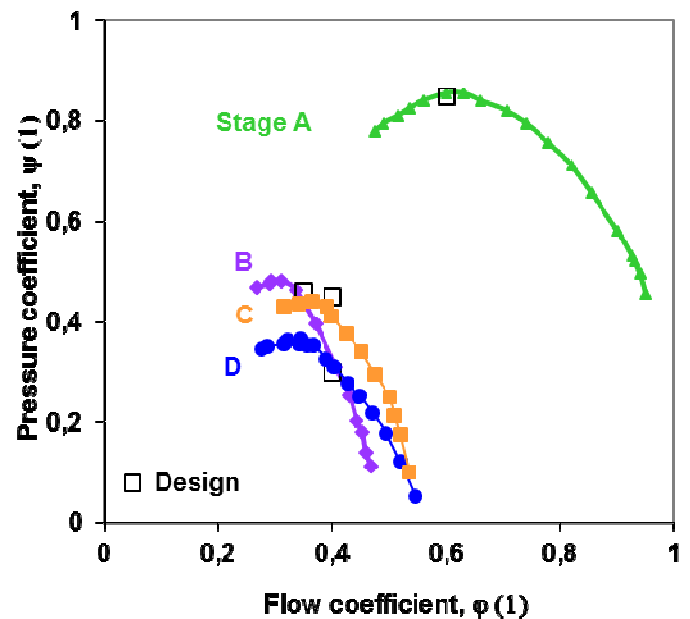
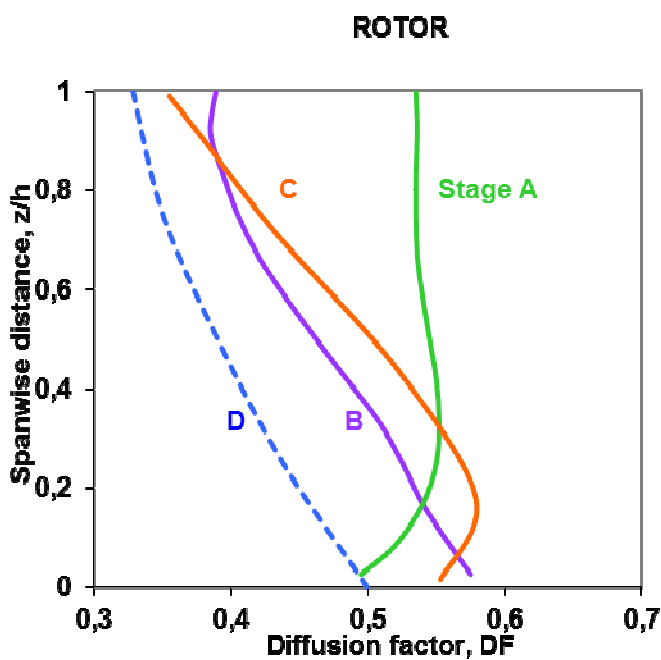


Figure 6: spanwise distribution of rotor diffusion factor

Figure 7: test curves of stage performance

The relative height of the radial clearance between the rotor blade tip and casing was $s_r/c = 0.008$. The ratio of tip clearance and fan diameter was $s_r/D_t = 0.0013$.

Axial flow stage aerodynamic performance

New stages were verified on 600 mm external diameter test rig, Cyrus et al [2], [3]. Tests were carried out at 1,800 1/min; this refers to the inlet Mach number of stage blade rows $Ma_1 < 0.30$ and the Reynolds number $Re = u_t c/\nu = 360 \times 10^3$. The uncertainty in calculating the fan stage efficiency κ_η in design condition was determined on the basis of uncertainty analysis $\kappa_\eta = \pm 1.0$ to 1.2 %. Test rig details and measurement method may be found in [2], [3].

Fig.7 shows relationship of the pressure coefficient ψ_{ST} and flow coefficient ϕ for all investigated stages. The design points are also shown. All stages had relatively high maximum efficiency $\eta_{ST,max} = 90.2\%$ to 91.1 %, thus we may conclude that the design objectives were met. Fan design methodology provided good results for highly aerodynamically loaded axial flow fan stages.

Further analysis of the aerodynamic performance of investigated stages working at different stagger angles of the rotor blades in the range of $\Delta\gamma_R = \pm 20^\circ$ was carried out. In Fig. 8 graphs of the test maximum pressure coefficient $\psi_{ST,max}$ for the discrete rotor blade stagger angles of high pressure Stages A, B,C and standard Stage D are compared. Maximum efficiency $\eta_{ST,max} = 85\%$ is denoted on graphs to determine good efficiency working regions.

It is evident that the Stage A and B working areas are side by side. It may be added that the maximum pressure lines of these stages determine the limits of the stage performance with the prescribed maximum efficiency $\eta_{ST,max} > 90\%$ for the hub/tip ratio of $\nu = 0.6$. For the Stage C with lower hub/tip ratio $\nu = 0.5$ we may observe the decrease of the maximum pressure coefficient $\psi_{ST,max}$ by 0.06 to 0.08 in comparison with the Stage B (Fig. 8).

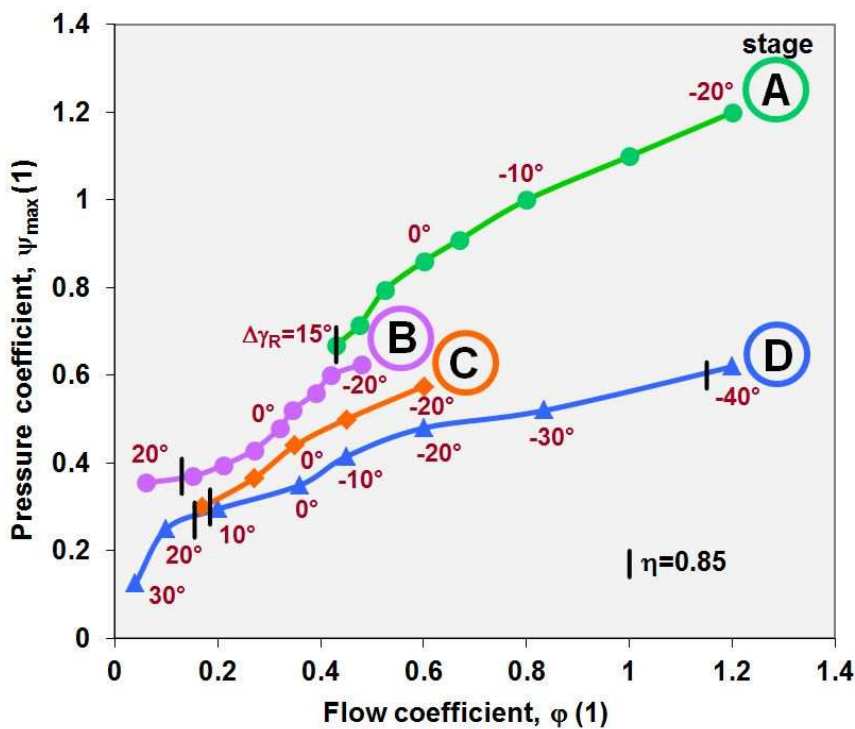


Figure 8 : dependences of maximum stage pressure coefficient on flow coefficient

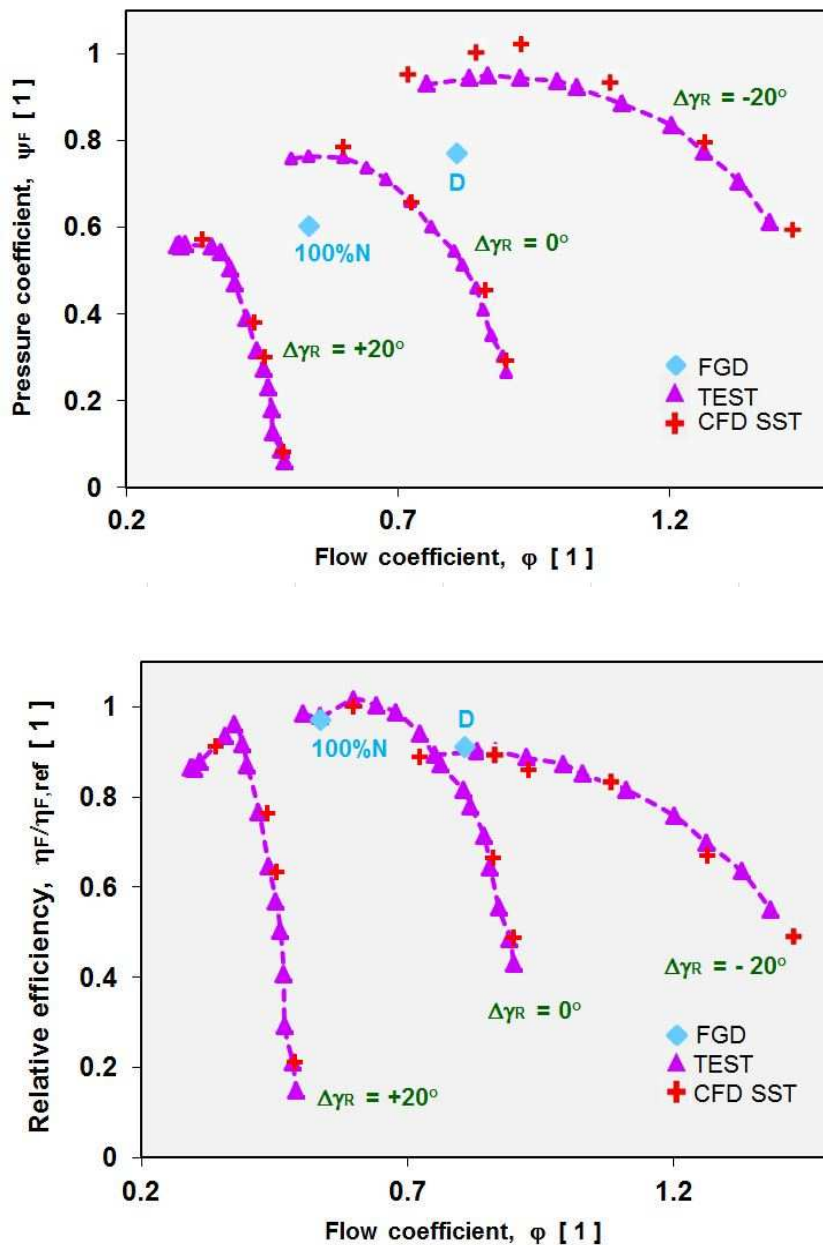


Figure 9 : comparison of computed and experimental fan performance ($D_t = 600$ mm)

The reason may be explained with the help of velocity triangles and basic relationships valid for the axial flow stage internal aerodynamics, for example in [10]. For the comparison the pressure coefficient $\psi_{ST,max}$ graph for the standard fan Stage D with moderate aerodynamic loading is also shown. Wide range of the flow coefficient values ϕ is apparent where the Stage D efficiency is relatively high $\eta_{ST,max} = 85\%$ to 90% and acquired in the wide range of the rotor blade stagger angles $\Delta\gamma_R = -38^\circ$ to $+15^\circ$. Such good aerodynamic performance is due to the lower aerodynamic loading of the stage cascades in contrast to high pressure Stages A, B and C.

We may assess the significant increase of the fan stage working range by the use of newly designed stages. The new stage aerodynamic characteristics allow optimising the design of modern axial fans in terms of production costs and attaining maximum pressure gain and efficiency. Their use may lead in some cases to the reduction of the peripheral axial flow fan's external diameter. Exceptionally, two-stage fan may be replaced by one-stage machine; such design measures save manufacturing costs.

Comparison of measured and calculated complete fan performance

One-stage axial flow fans were tested with new stages on the test rig built according to standard of ISO 5801[14]. Complete fan performance fields were measured for the rotor blades stagger angle range of $\Delta\gamma_R = \pm 20^\circ$. At the same time, the steady flow simulations using the CFD method (NUMECA program) were carried out to determine the fan characteristics. The turbulence model by SST was applied. The flow simulation conditions are published in more detail in papers [7] and [8].

Examples of comparison of tested and calculated fan aerodynamic performance are presented in Fig. 9. The dependencies of the pressure coefficient and relative efficiency on the flow coefficient are valid for one-stage fan with stage blading A. The exhaust diffuser had the area ratio of $A_4/A_3 = 1.87$ and the inlet chamber with parameters of $b/a = 1.28$ and $a/D_t = 1.25$. Rectangular side a was parallel to the fan axis (Fig. 1). The shape of the standard chamber is apparent from Fig. 1. Casing hub was supported by struts; the standard version had 5 short and thin (dashed line) and 3 long and thick struts (full line), refer to Fig. 1.

We may observe acceptable agreement between the test and calculation within the relatively large fan working range. Consequently, the aerodynamic performance of the inlet chamber and exhaust diffuser attained from the CFD data may be applied in our fan design study.

DESIGN STUDY OF ONE-STAGE FLUE GAS AXIAL FLOW FAN FOR THE HIGH OUTPUT COAL FIRED POWER STATION BLOCK

Our paper presents example of design optimisation of the flue gas axial fan destined for a large coal fired 660 MW power plant block. Required volume flow rate of the flue gas and fan specific work at the nominal point were $Q = 830 \text{ m}^3/\text{s}$ and $Y = 8,500 \text{ J/kg}$ or at the point of maximum flow $Q = 1,250 \text{ m}^3/\text{s}$ and $Y = 10,800 \text{ J/kg}$ (Fig. 2). Flue gas temperature in the fan inlet was 180°C . Use of standard stage with the hub ratio of 0.5, external diameter $D_t = 4.3 \text{ m}$ and circumferential velocity $u_t = 168 \text{ m/s}$ in two-stage fan was able to meet the assignment requirements. Electric motor revolutions were 745 1/min. Main fan parameters are presented in Table 2. This fan was manufactured and installed, one machine only, at the new modern brown coal boiler block in power station located in the Northern Bohemia.

Use of one standard Stage D or new high pressure Stages B and C in the design of investigated flue gas fan was not possible. Namely, the stage pressure coefficient values were too low at working points 100%N and D to meet design requirements, as it follows from Fig. 8.

For this reason we used Stage A with the hub/tip ratio of $v = 0.6$ in the flue gas fan design. Fan parameters are also presented in Table 2. The same values of external diameter $D_t = 4.3 \text{ m}$ and peripheral velocity $u_t = 168 \text{ m/s}$ are used.

The working points are marked by blue rhombi (flue gas fan notation – FGD) in the performance map of modelled one-stage axial flow fan with external diameter of 600 mm and blading A. Both typical points lie within the one-stage fan performance field. Particularly, the nominal point 100%N is located within the area of high efficiency $\eta_F = 83.4 \%$. (Fig. 9).

Comparison between the fan efficiency of one-stage fan at nominal points with the hub/tip ratio of 0.6 and two-stage fan with the hub/tip ratio of 0.5 for modelled dimensions $D_t = 600 \text{ mm}$ was carried out. The fan efficiency η_F was calculated according to the equation (2) with the following characteristics

One stage fan : $\zeta_{IC} + \zeta_D = 0.16, \varphi = 0.536, \eta_{F,1ST} = 0.843$

Two stage fan : $\zeta_{IC} + \zeta_D = 0.14, \varphi = 0.454, \eta_{F,2ST} = 0.866$.

The inlet chamber and diffuser loss coefficients were determined with the help of flow simulation data acquired in modelled axial flow fans with different hub/tip ratios. The sum of coefficients $\zeta_{IC} + \zeta_D$ was slightly lower for the fan with lower hub/tip ratio than for the fan with higher ratio.

The same values of the stage efficiency $\eta_{ST} = 0.90$ and pressure coefficient $\psi_{ST} = 0.73$ for both fans were used in calculation of the fan efficiency η_F . These were determined from tests results. The difference in fan efficiency $\Delta\eta_{F,th} = \eta_{F,2ST} - \eta_{F,1ST} = 2.3\%$ was calculated using equation (2). We should add to our analysis of two-stage machine that the deterioration in fan performance occurs because of the interaction of two-stage blading and additional energy losses due to struts usually located at the second stator blade row in order to increase bearings stiffness. This decrease may be estimated as $\Delta\eta_{F,c} = -0.5\%$ to -0.8% . Thus the estimated difference of fan efficiencies of two-stage standard fan and one-stage fan may be deduced as $\Delta\eta_F = \Delta\eta_{F,th} - \Delta\eta_{F,c} = 1.5\%$ to 1.8% . We assume that this difference value is the same for the modelled and prototype fan.

The structural analysis of the full size rotor blades was carried out using the MFE code. It was assumed that the blades were manufactured from the aluminum alloy with a special surface coating or from cast steel.

When estimating the prototype fan efficiency (external diameter of 4,300 mm) we used the measured results of modelled fan (external diameter of 600 mm) on the basis of similarity analysis. The Reynolds number Re_u and relative surface roughness k were used as similarity parameters [9]. This method suggests the following relationship between the efficiency values valid for the modelled fan $\eta_{F,M}$ and prototype η_F in working region near the design point

$$\eta_{F,M} - \eta_F = -(1 - \eta_{F,M}) \frac{c_{f,M} - c_f}{c_{f,M}}, \quad (5)$$

where c_f is the friction factor which is in the general function of relative roughness $k = K/c$ and Reynolds number Re . The method uses the boundary layer relations [9] valid for the entire region from the hydraulically smooth to hydraulically rough. For the axial flow stage the following definition of the Reynolds number is used

$$Re_u = u_t D_t / \nu \quad (6)$$

where ν is the gas kinematic viscosity. In Table 3 the key properties are given in order to determine the efficiency of full size one-stage axial flow fan η_F at a nominal point. This value $\eta_F = 89.4\%$, is higher than the one acquired on modelled fan and refers to typical values of the fan efficiency published by manufacturers. It should be added that this efficiency is only valid for new flue gas fan when no abrasion effect on the blade surface due to ash particles in flue gas is noticeable.

Table 2: flue gas fan parameters; $D_t = 4,300$ mm, $u_t = 168$ m/s

Working point	Q (m ³ /s)	Y (J/kg)	ψ_F (1)	φ (1)	
				$\nu = 0.6$	$\nu = 0.5$
100%N	830	8,500	0.604	0.536	0.454
D	1,250	10,800	0.768	0.808	0.684

Table 3: one-stage axial flow fan

	D_t (mm)	u_t (m/s)	Re_u (1)	Gas temperature t ($^{\circ}$ C)	K_R (μ m)	K_S (μ m)	η_F (1)
Model	600	56.5	2.2×10^6	18	5	6	0.834
Prototype	4,300	168	2.4×10^7	180	15 ⁺	25 ⁺	0.894

⁺ estimated

CONCLUSIONS

Modern coal fired stations blocks with electrical output of 500 to 800 MW require new axial flow fans with higher pressure increase and volume flow rate than currently available in existing standard machines. The paper had two main objectives. The first one focused on the analysis of high pressure coefficient fan stages design with high aerodynamic loading of the rotor and stator blade rows under the condition of maintaining the maximum stage efficiency of 90 %. Our test data relating to three new advanced model fan stages with external diameter of 600 mm were used. The stage hub/tip ratio was within the range of 0.5 to 0.6. Several relationships to determine the key fan parameters were derived. The second objective entailed the design study of advanced flue gas fan with the use of new high pressure fan stages for the power station block with output of 660 MW with the aim to replace two-stage fan by one-stage machine. The main conclusions are summarised as follows:

- (i) High efficiency fans should operate at nominal points with relatively low flow coefficient of 0.3 to 0.5. Their inlet chambers and exhaust diffusers should have low energy losses
- (ii) Objectives for all newly designed high pressure stages were met thus we concluded that the design methodology is trustworthy. Used design diffusion factor criterion for the rotor and stator rows cascades $DF_{max} < 0.58$ led to the maximum stage efficiency of $\eta_{ST,max} = 90\%$ to 91% as it follows from the modelled stage test data
- (iii) New stages significantly increased the fan stage working field in comparison to the standard stages
- (iv) Fans with new stages were tested using 600 mm external diameter model. The test and theoretical (CFD) fan performance was compared with good results, consequently theoretical data relating to the aerodynamic performance of stage blading, inlet chamber and exhaust diffuser were used for the design optimisation of the complete fan
- (v) New stages allow optimising the design of modern axial flow fans in terms of production costs and achieving the maximum pressure gain and efficiency
- (vi) Our paper deals with the design example of flue gas fan with the diameter of 4.3 m and peripheral velocity of 168 m/s destined for brown coal power plant block with electric output of 660 MW. Our design study showed that the original two-stage fan (hub/tip ratio 0.50) with standard moderate aerodynamic loading could be replaced by one-stage machine using new high pressure stage (notation A, hub/tip ratio 0.60, design pressure coefficient 0.83). Relatively small decrease in efficiency of 1.5 % to 1.8% was estimated.
- (vii) Efficiency of the full size one-stage fan at a nominal point was calculated with the use of the TU Darmstadt similarity method using the Reynolds number and relative roughness as similarity criteria on the basis of efficiency determined on modelled fan test data. Predicted prototype fan efficiency was higher by 6.0 % than for the modelled fan
- (viii) Theoretical and experimental research of the high pressure axial flow fans with high efficiency for new large output power station blocks should continue. Particularly, the decrease of

energy losses in the inlet chamber and exhaust diffuser is highly desirable. The design of new stages with low hub/tip ratio ($v = 0.4$ to 0.5) with good aerodynamic performance is also looked-for for the high volume flow fans

ACKNOWLEDGEMENTS

Research work was carried out for the ZVVZ Machinery. Authors wish to acknowledge the support and grants given by the Czech Ministry of Industry and Trade (MPO): No. 2A-1TP1/052 and FR-TII/347, Czech Technology (TACR) and Czech Grant Agency (GACR): No. TA04020228 and 14-08888S.

BIBLIOGRAPHY

- [1] S. Baumgarten, H. Krasmann, J. Roesener – *Stand der Forschung an aerodynamisch Hochbelasteten Axialventilatoren am Pfeleiderer Institute*, Mitteilungen TU Braunschweig, No.1, pp.147-160, **1994**
- [2] V. Cyrus – *Design of Axial Flow Fans with High Aerodynamic Loading*, Forschung im Ingenieurwesen-Engineering Research, Bd.62, Nr.3, S.58-64, **1996**.
- [3] V. Cyrus, P. Wurst – *High Pressure Axial Flow Fans for Power Industry*, Proceedings of 9th European Conf. on Turbomachinery Fluid Dynamics and Thermodynamics, pp. 81-93, Istanbul, **2011**
- [4] G.Sheard (editor), *Advances in industrial fans technology*. Sigel Press, Cambridge, **2012**
- [5] J.Vad - *Forward blade sweep applied to low-speed axial fan rotors of controlled vortex design:An overview*. Proceedings of ASME Turbo Expo 2012:ASME Paper No. GT2012-70103, June 11-15, 2012, Coopenhagen, Denmark, **2012**
- [6] C. Clemen, U. Stark., J. Fridrics., S. Baumgarten and G. Kosyna – *Effect of meanline shape, sweep and dihedral on stator performance of highly loaded single stage axial flow low-speed compressor*. Proceedings of 5th European conference on Turbomachinery Fluid dynamics and Thermodynamics, pp. 34-45, Lille, **2005**
- [7] V.Cyrus, J.Cyrus, P.Panek - *Design and Aerodynamic performance of a high pressure axial flow fan*. FAN 2012, International Conference on Fans, Senlis, (France), 18-20 April, **2012**
- [8] V.Cyrus,, J.Cyrus, P. Wurst, P. Panek - *Aerodynamic performance of advanced axial flow fan for power industry within its operational range*. Proceedings of ASME Turbo Expo 2014: Turbine conference and exposition, ASME Paper No. GT2014-25339, June 16-20, Dusseldorf, Germany, **2014**
- [9] P. F. Pelz and S. Stonjek – *Introduction of an universal scale-up method for the efficiency of axial and centrifugal fans*. Proceedings of ASME Turbo Expo 2014: Turbine conference and exposition, ASME Paper No. GT2014-25403, 16-20 June, Dusseldorf, Germany, **2014**
- [10] N. A.Cumpsty - *Compressor Aerodynamics*, Krieger, **2003**
- [11] V. Cyrus, V. Bruna, V. Folta, M. Sprinc, M.Lindova, I. Krasny et al - *A CADAC code for axial flow compressor stage design*. National Research Institute for Machine Design (SVUSS), Prague-Bechovice , 1995
- [12] S. Lieblein - *Experimental Flow in Two-dimensional Cascades*. NASA SP 36, p.183, **1966**
- [13] Numeca Manuals, **2013**
- [14] Industrial fans - Performance testing using standardized airways, ISO 5801, **1997**

LIST OF SYMBOLS

A	flow area	η	efficiency $\eta = Q \Delta p_T / (M_k \omega)$
AR	blade aspect ratio $AR = h/c$	σ	cascade solidity $\sigma = c/s$
c	chord	ϕ	flow coefficient $\phi = Q / (A u_t)$
DF	diffusion factor $DF = 1 - w_2/w_1 + ((w_{u1} - w_{u2})/2\sigma w_1)$	ψ	pressure coefficient $\psi = 2 \Delta p_T / (\rho u_t^2)$
D	diameter	ω	angular velocity
h	blade height	ρ	density
K	roughness height		
M_k	torque		
p_T	total pressure		
Q	volume flow rate		
r	radius		
s	blade pitch		
u_t	peripheral velocity at casing		
w	velocity		
Y	fan work $Y = \Delta p_T / \rho$		
z	coordinate normal to hub, blade number		
ζ	loss coefficient		
v	hub/tip ratio, kinematic viscosity		

Indexes

F	fan
D	design, diffuser
h, t	hub, tip
IC	inlet chamber
M	model
R	rotor
S	stator
ST	stage (rotor + stator)
u	peripheral
1,2	inlet, outlet

Abbreviations

BMCR	boiler maximum continuous rating fan operating point
D	maximum flow rate fan operating point
FGD	flue gas fan
MFE	finite elements method
SST	turbulence model [13]